Five-Membered Ruthenacycles Ligand-Assisted Alkyne Insertion into 1,3-N,S-Chelated Ruthenium Borate Species

Mohammad Zafar, Rongala Ramalakshmi, Kriti Pathak, Asif Ahmad, Thierry Roisnel, Sundargopal Ghosh

10.1002/chem.201902663

WILEY-VCH

Five-Membered Ruthenacycles: Ligand-Assisted Alkyne Insertion into 1,3-*N,S*-chelated Ruthenium Borate Species

Mohammad Zafar,[a] Rongala Ramalakshmi,[a] Kriti Pathak,[a] Asif Ahmad,[a] Thierry Roisnel,[b] Sundargopal Ghosh*[a]

Dedicated to Prof. Jean-François Halet on the occasion of his 60th birthday

Abstract: Building upon our earlier work, we have extended the chemistry of [(η^6-*p*-cymene)Ru{P(OMe)$_2$OR}Cl$_2$], (R = H or Me) with [H$_2$B(mbz)$_2$]$^-$ using different Ru-precursors and borate ligands. As a result, a series of 1,3-*N,S*-chelated ruthenium borate complexes, for example, [(κ^2-*N,S*-L)PR$_3$Ru{κ^3-H,S,S′-H$_2$B(L)$_2$}], (**2a-d** and **2a'-d'**; R = Ph, Cy, OMe or OPh and L = C$_5$H$_4$NS or C$_7$H$_4$NS$_2$) and [Ru{κ^3-H,S,S′-H$_2$B(L)$_2$}$_2$], (**3**: L = C$_5$H$_4$NS, **3'**: L = C$_7$H$_4$NS$_2$) were isolated on treating [(η^6-*p*-cymene)RuCl$_2$PR$_3$], **1a-d** (R = Ph, Cy, OMe or OPh) with [H$_2$B(mp)$_2$]$^-$ or [H$_2$B(mbz)$_2$]$^-$ ligands (mp = 2-mercaptopyridyl; mbz = 2-mercaptobenzothiazolyl). All the Ru-borate complexes, **2a-d** and **2a'-d'** are stabilized by phosphine/phosphite and hemilabile *N,S*-chelating ligands. Treatment of these Ru-borate species, **2a'-c'** with various terminal alkynes yielded two different types of five-membered ruthenacycle species, namely [PR$_3${C$_7$H$_4$S$_2$-(*E*)-N-C=CH(R')}Ru{κ^3-H,S,S'-H$_2$B(L)$_2$}], (**4-4'**; R = Ph and R' = CO$_2$Me or C$_6$H$_4$NO$_2$; L = C$_7$H$_4$NS$_2$) and [PR$_3${C$_7$H$_4$NS-(*E*)-S-C=CH(R')}Ru{κ^3-H,S,S'-H$_2$B(L)$_2$}], (**5-5'**, **6** and **7**; R = Ph, Cy or OMe and R' = CO$_2$Me or C$_6$H$_4$NO$_2$; L = C$_7$H$_4$NS$_2$). All these five-membered ruthenacycle species contain an exocyclic C=C moiety, presumably formed by the insertion of a terminal alkyne into the Ru-N and Ru-S bonds. The new species have been characterized spectroscopically and the structures were further confirmed by single-crystal X-ray diffraction analysis. Theoretical studies and chemical bonding analyses established that charge transfer occurs from phosphorus to ruthenium centre following the trend PCy$_3$<PPh$_3$<P(OPh)$_3$<P(OMe)$_3$.

Introduction

Metal-based complexes having donor ligands are of great interest in catalysis and organometallic chemistry.[1] In some cases, the ligand systems actively participate to tune the coordination of the metal facilitating new reaction pathways.[2] In recent times, metal-ligand cooperativity (MLC) has been broadly explored for many organic tranformations, such as water splitting, C-H activation and hydrogenation of organic compounds.[2-6] MLC may proceed *via* hemilabile,[7] redox-active[2,8] or bifunctional ligands.[4f,9] The hemilabile ligands, in particular, have been of significant interest as they stabilize the metal coordination by chelation and change the denticity to facilitate proton migrations allowing key bond cleavage and/or formation.[2-6] On the other hand, activation of C-H bond with regioselective and specific functionalization, continues to be an area of intense research.[6,10] For example, palladium-group metals containing 1,3-donor acetate ligands could be employed for activation of C-H bond of hydrocarbons *via* ambiphilic metal-ligand activation (AMLA).[11] Likewise, recently Schafer and coworkers reported that the 1,3-N,O-chelated phosphoramidate Cp*Ir(III) complex, [Cp*Ir(κ^2-N,O-Xyl(N)P(O)(OEt)$_2$][BAr$^F_4$] (Xyl = 2,6-Me$_2$C$_6$H$_3$; Ar^F = 3,5-(CF$_3$)$_2$C$_6$H$_3$) is capable of activating terminal alkynes *via* MLC.[12] Very recently, Maseras et al. established that ruthenium complexes [Ru(X)H(CO)(P*i*Pr$_3$)$_2$] (X = κO$_2$-OC(O)Me or Cl) could be utilized for the activation of alkyne C-H bond through proton shuttle followed by a concerted metalation deprotonation (CMD).[13] The activation of terminal alkynes by ruthenium and iridium complexes has also been established through ligand-assisted proton shuttle (LAPS) mechanism;[10c,13-15] the LAPS mechanism for some alkyne-vinylidene tautomerizations has been proposed in Scheme 1.[10c]

Although, a variety of transition metal boron complexes are known in the literature,[16-18] their chemistry with small organic molecules has not been explored.[19-22] As a part of our ongoing research, we have explored the reactivity of various transition

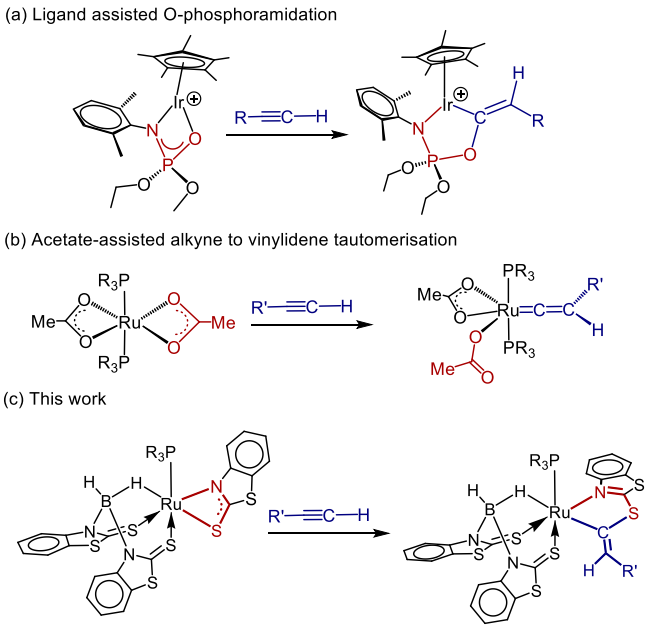

Scheme 1. Examples of activation of terminal alkynes using 1,3-bidentate ligands involving various mechanisms (a) and (b); this work (c).

[a] Mr. Mohammad Zafar, Dr. Rongala Ramalakshmi, Ms. Kriti Pathak, Mr. Asif Ahmad, and Prof. Sundargopal Ghosh
Department of Chemistry,
Indian Institute of Technology Madras, Chennai – 600036, India.
E-mail: sghosh@iitm.ac.in
[b] Dr. Thierry Roisnel
Univ Rennes, CNRS,
Institut des Sciences Chimiques de Rennes,
UMR 6226, F-35042 Rennes, France.
Supporting information for this article is given via a link at the end of the document.

metal boron complexes with alkynes.[19a,c,d,20-21] Likewise, in the course of our study, we have recently found that ruthenium borate complex [($PPh_2CH_2PPh_2$)Ru(κ^1-S,S'-$H_2B(L)_2$] (L = $C_7H_4NS_2$) yields different vinyl borane species when treated with terminal alkynes.[22] Herein this article, we report the synthesis and structural characterization of a series of *N,S*-chelating pyridyl/benzothiazolyl Ru-borate complexes and their reactivity with various terminal alkynes.

Results and Discussion

With the objective to study the reactivity of Ru-borate complexes with terminal alkynes, a series of 1,3-*N,S*-chelating mercapto-pyridyl borate complexes, [(κ^2-*N,S*-L)PR_3Ru{κ^3-H,S,S'-$H_2B(L)_2$}] (**2a**: R = Ph, **2b**: R = Cy, **2c**: R = OMe, **2d**: R = OPh; L = C_5H_4NS) and bis-borate species, [Ru{κ^3-H,S,S'-$H_2B(L)_2$}$_2$], (**3**: L = C_5H_4NS) were synthesized from the treatment of [(η^6-*p*-cymene)$RuCl_2PR_3$], (**1a**: R = Ph; **1b**: R = Cy, **1c**: R = OMe; **1d**: R = OPh) with [$H_2B(mp)_2$]$^-$ (mp = 2-mercaptopyridyl) borate ligand (Scheme 2). The borate species **2a-d** are presumably formed by ruthenium induced B-N bond cleavage of [$H_2B(mp)_2$]$^-$ ligands.[23]

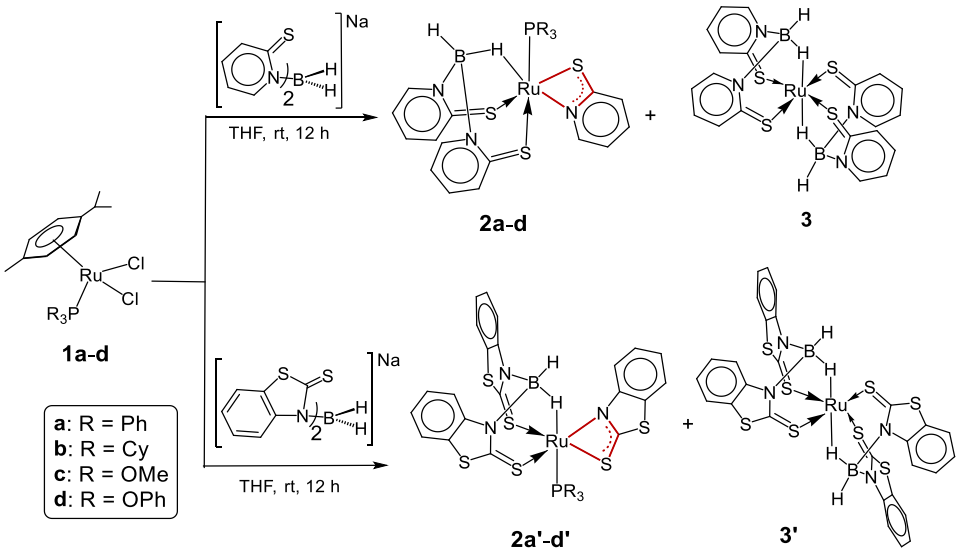

Scheme 2. Synthesis of *N,S*-chelating mercaptopyridinyl/benzothiazolyl borate complexes of ruthenium and ruthenium bis-borate complexes.

All the compounds have been characterized by multinuclear NMR and IR spectroscopy and mass spectrometry. The $^{31}P\{^1H\}$ NMR spectra of **2a-d** feature a singlet in the region of δ = 43.2 – 146.2 ppm and the $^{11}B\{^1H\}$ NMR spectra show a sharp peak in the region of δ = 7.7 – 10.1 ppm. Besides the presence of phospine/phosphite and mercaptopyridinyl ligands, the ^1H NMR spectra of **2a-d** provide chemical shifts for B-H and Ru-H-B protons in the range of δ = 3.60 to 4.54 and -14.61 to -15.48 ppm respectively. The IR spectra exhibit stretching frequencies in the region of 2195-2033 cm^{-1} for the Ru-H-B and 2496-2435 cm^{-1} due to the B-H bond. Further, the mass spectrometric data showed molecular ion peaks corresponding to species **2a-d** (Figures S1-S4). The solid-state X-ray diffraction analyses of suitable single crystals of **2a** and **2b** confirmed their molecular structures.[24]

Single crystals of **2a** and **2b** suitable for X-ray diffraction analyses were obtained from the slow diffusion of a hexane-CH_2Cl_2 solution. While **2a** crystallizes in the monoclinic system with *P2$_1$/n* space group, **2b** crystallizes in the triclinic system with *P-1* space group. The asymmetric unit of **2b** contains two independent molecules in the unit cell having similar structure. Thus, the structural data presented and discussed here is for one of the molecules. As shown in Figure 1, the geometry of **2a** and **2b** around the Ru center is distorted octahedral. Note that, although the bridging H atom in **2b** could not be located by X-ray diffraction analysis, ^1H NMR spectrum confirms the presence of this hydrogen. The bite angles (N-Ru-S) for the four-membered chelate rings in **2a** and **2b** are 67.64(12)° for **2a** and 67.4(2)° for **2b**. The torsion angle of the four-membered Ru-S-C-N ring for **2a** (2.2(4)°) is markedly larger as compared that for **2b** (-3.5(5)°). The Ru-B distance of 2.505(6) Å for **2a** is shorter as compared to that for **2b** (2.554(9) Å) and other reported borate complexes, for example, [Cp*Ru{κ^3-H,S,S'-$H_2B(L)_2$}] (2.753(1) Å)[17a] and [(cod)ClRu{κ^3-H,S,S'-$H_2B(L)_2$}] (2.697(4) Å)[17c] (L = $C_7H_4NS_2$). In line with the substitution of R = Ph in **2a** to R = Cy in **2b**, the Ru-P distance is found to be longer in **2b** (2.3573(19) Å) as compared to that in **2a** (2.3124(13) Å). Notably, the Ru-S bond distances [2.3951(14) Å for **2a** and 2.400(2) Å for **2b**] *trans* to the Ru-P bond are significantly longer than other Ru-S bond distances in **2a** (2.3336(13) Å) and **2b** (2.327(2) Å) due to *trans* influence. The other bond lengths such as Ru-N and B-N are comparable with other reported species.[17a-b,18a,19]

Similarly, as shown in Scheme 2, treatment of **1a-d** with [$H_2B(mbz)_2$]$^-$ led to the formation of *N,S*-chelating Ru-species, [(κ^2-*N,S*-L) PR_3Ru{κ^3-H,S,S'-$H_2B(L)_2$}], (**2a'**: R = Ph, **2b'**: R = Cy, **2c'**: R = OMe[19d], **2d'**: R = OPh[19d]; L = $C_7H_4NS_2$). The chelating complexes were isolated as crystalline solids and were characterized by ^1H, $^{11}B\{^1H\}$, $^{13}C\{^1H\}$, $^{31}P\{^1H\}$, IR spectroscopy and in some cases by X-ray crystallographic analyses. The molecular ion peaks in the mass spectrometric data further confirm the formulation of **2a'-b'** (Figures S6 and S7).

The spectroscopic data[25] and the mass spectrometric analyses suggest that **2a'-d'** are analogous to **2a-d**. This is further confirmed by the X-ray crystallographic analysis of a red, rectangular-shaped crystal of **2a'**. The solid-state structure of **2a'** (Figure 1c) corroborates with the spectroscopic data and the core geometry is similar to **2a** with the borate ligands being the distinctive difference between the two structures. The bidentate

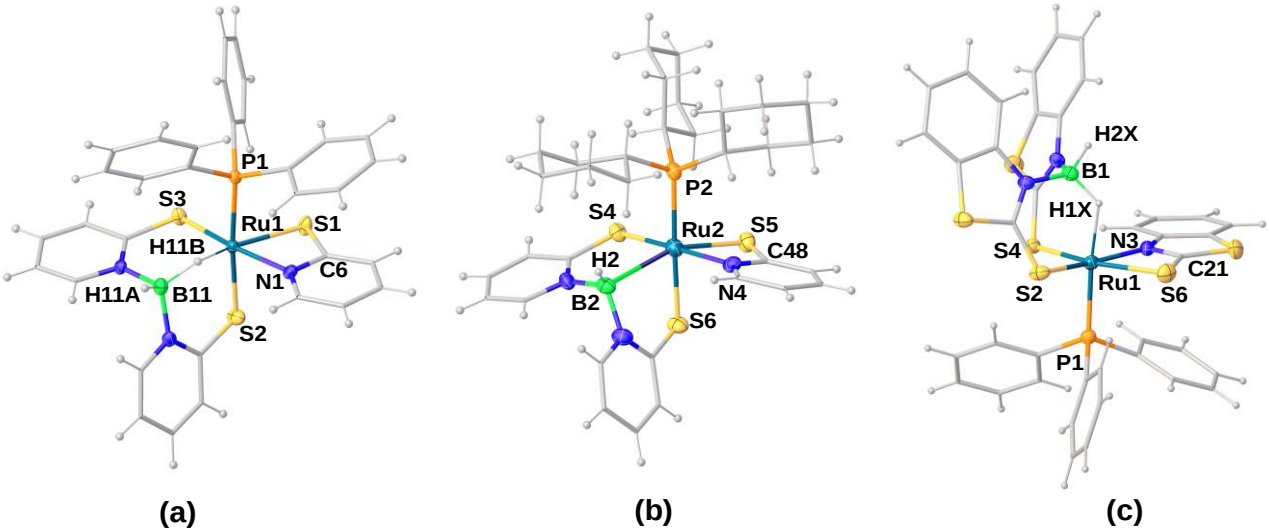

Figure 1. Molecular structures of **2a**, **2b** and **2a'**. Selected bond lengths (Å) and angles (°). **2a** (a): Ru1-H11B 1.65(7), Ru1-B11 2.505(6), Ru1-S1 2.4253(13), Ru1-S2 2.3951(14), Ru1-S3 2.3336(13), Ru1-N1 2.099(4), Ru1-P1 2.3124(13), S1-C6 1.737(6), C6-N1 1.351(7), B11-H11B 1.32(7), N1-Ru1-S1 67.64(12), P1-Ru1-S1 88.59(5), N1-Ru1-P1 91.79(13), Ru1-N1-C6 102.5(3); N1-C6-S1 109.6(4). **2b** (b): Ru2-B2 2.554(9), Ru2-P2 2.3573(19), Ru2-S4 2.327(2), Ru2-S5 2.452(2), Ru2-S6 2.400(2), Ru2-N4 2.075(7), S5-C48 1.700(11), C48-N4 1.367(10), B2-H2 0.9800; N4-Ru2-S5 67.4(2), P2-Ru2-S5 95.82(7), N4-Ru2-P2 93.94(18), Ru2-N4-C48 102.2(6). **2a'** (c): Ru1-H1X 1.88(4), Ru1-S2 2.3268(18), Ru1-S4 2.3469(16), Ru1-S6 2.4741(18), Ru1-N3 2.135(5), Ru1-P1 2.2696(15), S6-C21 1.744(7), C21-N3 1.320(7), B1-H1X 1.22(4), B1-H2X 1.08(5); N3-Ru1-S6 67.08(13), P1-Ru1-S6 90.84(6), Ru1-N3-C21 100.0(4); N3-C21-S6 114.9(5).

N,S-donor group forms a four membered chelate ring with a bite angle of 67.08(13)˚, comparable to that of [$(PPh_3)_2$)Ru(*N,S*-mbz)$_2$)] (67.295(11)˚).[26] The Ru1-S6-C21-N3 ring is almost flat with a torsion angle of -0.7(5)˚, larger than that of **2d'** (-3.5(4)˚).[19d] The Ru1-S6 bond distance of 2.4741(18) Å in **2a'** is significantly longer compared to Ru1-S2 and Ru1-S4 bond distances in **2a'** (2.3268(18) and 2.3469(16) Å respectively) and other ruthenium complexes.[27] The Ru-B distance of 2.755 Å in **2a'** is significantly longer as compared to **2a** (2.505(6) Å) and [ClRu(cod){κ^3-H,S,S′-H_2B(mbz)$_2$}] (2.697(3) Å).[17c]

Computational analytical methods based on the density functional theory (DFT), natural bond orbital (NBO) analysis and quantum theory of atoms and molecules (QTAIM) model were employed in order to gain some insight into the electronic structure and nature of bonding of the complexes **2a**-**d** and **2a'**-**d'**. The bond lengths of the optimised structures at the ground state are in well agreement with the experimental values (Table S1). The ^{11}B and ^{1}H chemical shifts computed by gauge-including atomic orbitals (GIAOs) method, also well corroborate with the experimental values (Table S3). The Kohn-Sham orbitals of all these molecules show that the HOMOs are mainly localized on the d-orbital of ruthenium and the p-orbitals of nitrogen and sulphur atoms of the borate ligands. The LUMOs are mainly found to be localized over the pyridyl/ benzothiazolyl moities (Figure S62). The natural bond orbital (NBO) analysis show that the transfer of charge occurs from phosphorus to the ruthenium centre in all the complexes. This charge transfer follows the trend PCy_3<PPh_3<$P(OPh)_3$<$P(OMe)_3$ and is found to be greater in **2'** than in **2**. Hence, while the natural charges of P atoms are positive, the Ru atoms bear negative charges for all molecules (Table S2) due to the charge transfer. The donation of the phosphorus atom lone pair to ruthenium has further been supported by the increase in the natural valence population at ruthenium marked by a decrease over the phosphorus atoms (Table S2). In addition, the NBO analysis also indicate the Ru-H- B bonding interaction (Figure

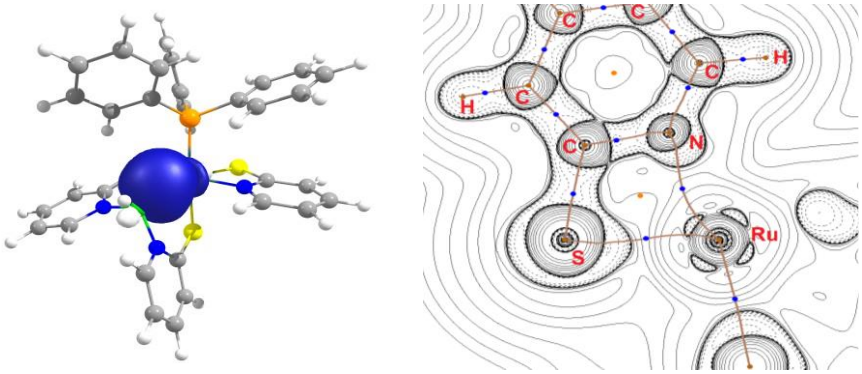

Figure 2. (a) The Ru-H-B bonding interaction obtained from NBO analysis at an isovalue of 0.04 $a_0^{-3/2}$. (b) Contour-line diagram of the Laplacian of electron density of **2a** in the RuSCN plane. The solid brown lines are bond paths, while red and blue spheres indicate the ring and bond critical points. Areas of charge concentration [$\nabla^2\rho(r)<0$] are indicated by solid lines and areas of charge depletion [$\nabla^2\rho(r)>0$] are shown by dashed lines.

2a). Further, the Wiberg bond index (WBI) analysis show a strong bonding interaction between ruthenium and phosphorus which is maximun in **2d**. A similar trend has also been observed for **2a'**-**2d'** (Table S1).

The topologies of the molecules were analysed by the quantum theory of atom in molecules (QTAIM) approach in order to probe the presence of the Ru-P and Ru-H-B bonds. In each case, the existence of (3, -1) bond critical points (BCPs) indicate the presence of Ru-P and R-H-B bonds. As shown in Table S4, the Ru-P interactions are mostly closed-shell in nature with electron density (ρ) in the range of 0.081-0.102, positive Laplacian values ($\nabla^2\rho$) are in between 0.215-0.326 and the negative energy density (H) varies from -0.021 to -0.035 at BCPs. On the other hand, the BCP data between Ru and H-B show characteristics of polar bond. The Laplacian of the electron density at the Ru-S bonds in **2a** are positive and they decreased with the increase of bond length that suggest polar covalent nature of the bonds. A similar trend has also been observed for the Ru-S bonds in **2b**-**2d** and **2a'**-**2b'** (Table S4). In addition, contour plot of the Laplacian of the electron density ($\nabla^2\rho$) shows the presence of a ring critical point (RCP) in the RuSCN plane of **2a** thereby supporting the existence of the four membered RuSCN ring (Figure 2b), similar RCPs were found for the other molecules (Figures S63 and S64).

Reactivity of Ru-borate complex 2a'-c' with terminal alkynes

Hemilability is a form of metal-ligand cooperativity (MLC) in which either the electron donor or the acceptor moieties undergo a reversible dissociation. This allows the coordination environment at the metal center to be accordingly modified in order to meet the steric and electronic requirements of different reaction intermediates during the course of a catalytic reaction.[2-4,28] Thus, in order to probe the hemilabile character of 1,3-*N*,*S*-chelating mercaptopyridyl moiety attached to ruthenium, we carried out the reaction of **2a** with methyl propiolate. Unfortunately, the reaction led to decomposition of the starting material. However, as shown in Scheme 3, mild thermolysis of **2a'** with methyl propiolate and 1-ethynyl-4-nitro-benzene yielded two different kinds of complexes, **4**-**4'** and **5**-**5'**. Note that, under similar reaction conditions, **2b'** and **2c'** yielded **6** and **7** respectively as sole product. After chromatographic purification and crystallization from toluene/CH_2Cl_2, they were analyzed as ruthenium-alkenyl complexes, [PPh_3{$C_7H_4S_2$-(*E*)-N-C=CH(R')}Ru{κ^3-H,S,S'-$H_2B(L)_2$}], **4** and **4'** (**4**: R' = CO_2Me and **4'**: R' = $C_6H_4NO_2$; L = $C_7H_4NS_2$) and [PR_3{C_7H_4NS-(*E*)-S-C=CH(R')}Ru{κ^3-H,S,S'-$H_2B(L)_2$}], **5**, **5'**, **6**-**7** (**5**: R = Ph, R' = CO_2Me; **5'**: R = Ph, R' = $C_6H_4NO_2$; **6**: R = Cy, R' = CO_2Me; **7**: R = OMe and R' = CO_2Me; L = $C_7H_4NS_2$). Further, as shown in Scheme 3, under thermolytic conditions, compound **4** or **4'** can be converted to **5** or **5'**. Also, these Ru-borate species do not react with phenyl acetylene nor any internal alkynes under thermolytic or photolytic conditions. Thus, we believe that only terminal alkynes containing electron-withdrawing groups are feasible for this kind of reactions.

All the ruthenium-alkenyl complexes were fully characterized by NMR, IR spectroscopy, mass spectrometry and in some cases by X-ray crystallographic analyses. The $^{11}B\{^1H\}$ NMR spectra show a broad peak in the upfield region (Table 1). The ^1H as well as the $^{13}C\{^1H\}$ chemical shift values for all the species clearly indicate the presence of olefinic proton and carbon respectively. In addition to the presence of mbz ligands, their ^1H NMR spectra also show an upfield resonance in the region δ = -6.05 to -7.04 ppm (Table 1), which may be assigned to their Ru-H-B protons. The ^{31}P chemical shift of these species are slightly up-field shifted compared to their parent molecules. Furthermore, the $^1H\{^{13}C\}/^{13}C\{^1H\}$ HSQC experiment for one of these species, (**5**), confirms the presence of the vinyl CH group (Figure S47) in complexes **4**-**7**.

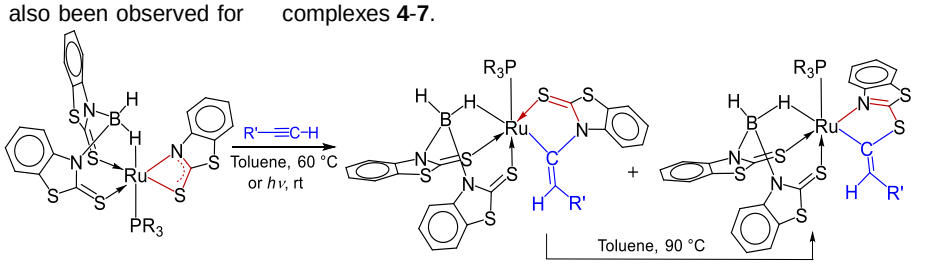

2a': R = Ph
2b': R = Cy
2c': R = OMe

4: R = Ph; R' = CO_2Me
4': R = Ph; R' = $C_6H_4NO_2$
5: R = Ph; R' = CO_2Me
5': R = Ph; R' = $C_6H_4NO_2$
6: R = Cy; R' = CO_2Me
7: R = OMe; R' = CO_2Me

Scheme 3. Generation of five membered ruthenium-alkenyl complexes from **2'** with terminal alkynes.

Table 1. Selected ^1H, ^{11}B, and ^{31}P chemical shift values of ruthenium-alkenyl complexes **4**-**4'**, **5**-**5'**, **6** and **7**

Ru-alkenyl species	$^{31}P\{^1H\}$ δ[a]	$^{11}B\{^1H\}$ δ[a]	^1H (Ru-*H*B) δ[a]	^1H (*H*C=C) δ[a]
4	51.9	-4.8	-6.70	6.72
4'	52.2	-5.2	-7.04	6.77
5	48.8	-4.3	-5.89	6.42
5'	50.8	-4.5	-6.16	6.76
6	38.0	-4.6	-6.05	6.91
7	144.3	-5.4	-6.48	6.76

[a] NMR spectra recorded in $CDCl_3$ solvent.

In order to illustrate the bonding and geometries of some of these species, the X-ray diffraction studies of **4, 5** and **5'** were carried out. The X-ray quality crystals were obtained from a toluene/ CH_2Cl_2 solution at room temperature. The solid-state X-ray structures of **4, 5** and **5'**, shown in Figure 3, clearly show the

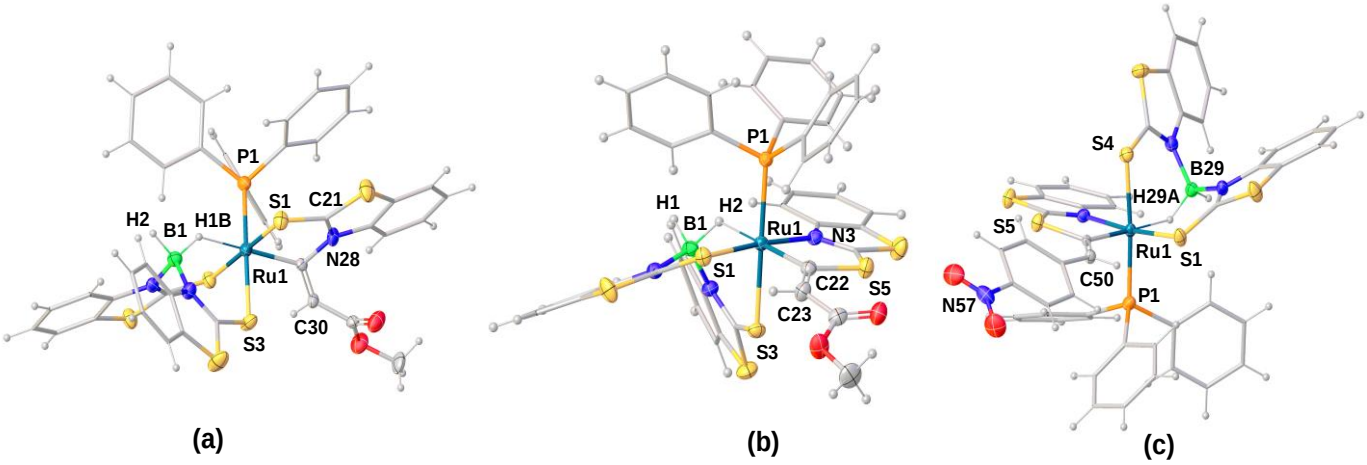

Figure 3. X-ray crystal structures of **4**, **5** and **5'**. Selected bond lengths (Å) and angles (°). **4** (**a**): Ru1-S1 2.3651(9), Ru1-S3 2.4286(9), Ru1-C29 2.021(3), C29-C30 1.356(5), C29-N28 1.466(4), C21-N28 1.353(5), C21-S1 1.675(4), Ru1-P1 2.3142(9), C30-C31 1.472(5), Ru1-H49B 1.86(4), C29-N28-C21 117.7(3), N28-C21-S1 121.4(3), C29-Ru1-S1 83.00(9); **5** (**b**): Ru1-N3 2.106(2), Ru1-C22 2.033(3), C22-C23 1.360(4), C22-S5 1.797(3), C21-S5 1.725(3), C21-N3 1.314(3), C23-C24 1.462(3), Ru1-P1 2.3236(7), Ru1-H2 1.82(4), B1-H2 1.25(4), Ru1-C22-S5 115.95(13), N3-C21-S5 124.7(2). **5'** (**c**): Ru1-N41 2.0963(19), Ru1-C49 2.027(2), C49-C50 1.354(3), C48-S12 1.720(2), C49-S12 1.795(2), C48-N41 1.319(3), C49-C50 1.354(3), Ru1-P1 2.3105(6), Ru1-S1 2.3288(6), Ru1-H29A 1.85(3), B29-H29A 1.19(3), B29-H29B 1.13(3); Ru1-C49-S12 115.25(12), N41-C48-S12 123.12(18).

conversion of the four-membered ring in **2a'** to five-membered metallacycles with an exo C=C double bond. Interestingly, the five-membered ring in **4** has a non-planar RuCNCS unit however, a planar RuCSCN unit exists in **5** and **5'**. From the molecular structures and formulae, **4** and **5** may be considered as structural isomers. The Ru-S1 and Ru-N3 distances of 2.3651(9) Å and 2.106(2) Å respectively are comparable with their parent molecule **2a'**. The Ru1-C29 and C29-C30 bond lengths of 2.021(3) and 1.356(5) Å respectively in **4** are in good agreement with the corresponding bonds of **5** (2.033(3) Å and 1.360(4) Å) and other Ru-vinyl complexes.[19b,29] The Ru1-P1 bond distances of 2.3142(9), 2.3236(7) and 2.3105(6) Å in **4**, **5** and **5'** respectively, are significantly longer as compared to **2a'** (2.2696(15) Å) suggesting a bond elongation upon insertion of alkyne moieties.

Metal catalysed N or S nucleophilic addition across the C-C triple bond has emerged as a suitable method for the synthesis of enamines or vinyl sulfides and their derivatives.[30,31] In this regard, Rh and Ru metals are found to be active catalysts for the addition of N or S nucleophiles to terminal alkynes yielding C-N or C-S bonds, mostly *via* anti-Markovnikov addition.[14,30,32] Hence, the formation of **4**-**5** or **6**-**7** might be thought to have occurred via initial activation of the alkyne followed by the proton transfer from alkyne to the basic *N,S*-benzothiazolyl group and a subsequent intramolecular anti-Markovnikov addition of N or S, of the benzo-thiazolyl moiety to the alkyne. The reactions might proceed through ligand assisted proton shuttle (LAPS) mechanism in which the nucleophilic sites, N or S, of the benzothiazolyl moiety in **2a'** would act as the internal base for proton shuttling thereby assisting both in the C-H bond activation as well as in the formation steps. The generation of five-membered metallacycles (**4**, **5** or **5'**) is very similar to the formation of five membered (*E*)-vinyloxy iridium(III) complex,[12] which also occurred via LAPS mechanism,[15a] as reported by Love and Schafer. This led us to believe that the insertion of terminal alkynes into Ru-N and Ru-S bonds of **2a'** follows LAPS mechanism, which facilitates the formation of C-N and C-S bonds (Scheme 4).[15a]

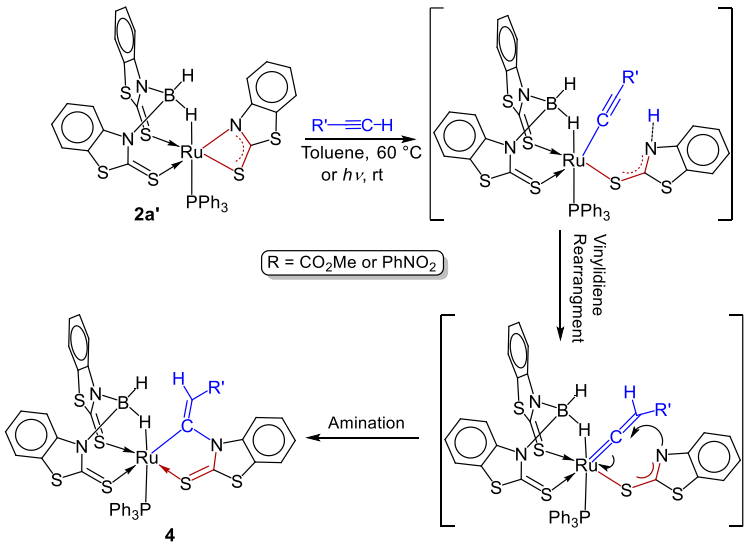

Scheme 4. Proposed mechanism for the generation of five membered ruthenium(II) cycle.

10.1002/chem.201902663

The calculated HOMO-LUMO energy gaps for **4** and **5** are slightly higher than that of parent **2a'** (**4** = 1.96 eV, **5** = 1.93 eV and **2a'** = 1.72 eV; Table S2). The HOMO-1 of **4** and **5** suggest the existence of C-C double bond, which is further supported by the WBI values obtained from NBO analyses (1.64 for **4** and 1.67 for **5**; Figures 4, S66 and Table S1). Further, the natural charges at Ru center in **5**-**7** are less than that at **4**. A similar trend has also been observed for natural valence population on Ru centre (Table S2). In addition, the Laplacian of the electron density plots for **4** and **5** in Ru-C-C plane provide similar electron density at bcp of C=C bond. In order to identify the electronic effect of alkyne, we have carried out calculations with normal alkyne which reveal that the C≡C antibonding π-orbital of alkynes containing electron withdrawing groups is lower in energy (0.065 eV) as compared to those of normal alkynes.

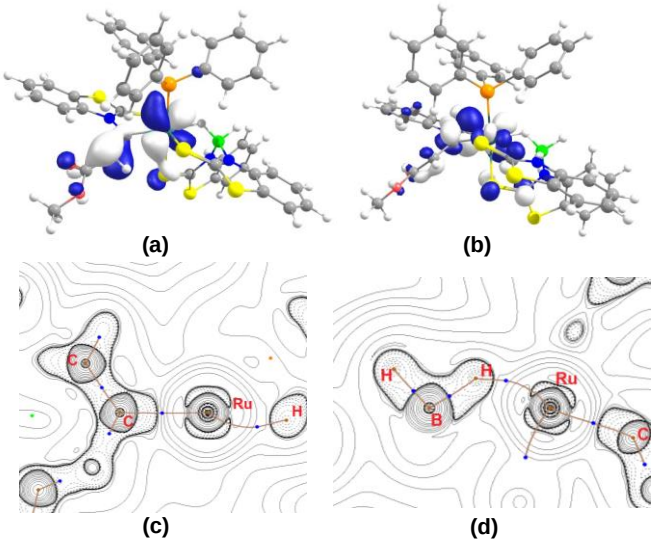

Figure 4. (a) and (b) Molecular orbitals (HOMO-1 and LUMO+2) involving C=C bonding and antibonding interactions of **4**; (c) and (d) Topology of the Laplacian of the electron density in Ru-C-C and Ru-H-B planes of **4** (positive charge emphasized in solid lines, negative charge in dashed lines, bcps in blue.

Conclusions

In this article, we have described the synthesis and characterization of a series of 1,3-*N,S*-chelated ruthenium borate complexes. Further, the reactivity of these borate complexes with terminal alkynes was carried out that yielded two five-membered ring Ru-CNCS and Ru-CSCN rythenacycles, featuring an exocyclic C=C double bond. We believe that these isomeric five-membered Ru-alkenyl species are formed through the insertion of alkyne into the Ru-N and Ru-S bonds of the hemilabile 1,3-*N*,*S* chelating benzothiazolyl moieties. The hemalibilty of 1,3-heterobidentate chelating ligand opens up new possibilities for the design of novel tuneable coordinate complexes that may be useful for metal based catalysis.

Experimental Section

All manipulations were conducted by using standard Schlenk line and glove box techniques under an atmosphere of dry argon. Solvents such as toluene, hexane and THF were distilled through Na/benzophenoneketyl and DCM was dried over calcium hydride prior to use under argon. $CDCl_3$ was degassed by three freeze-thaw cycles, dried over calcium hydride for 12 h, and stored over 4 Á molecular sieves in a Young's ampoule under argon. Compounds [(η^6-*p*-cymene)$RuCl_2PR_3$] (R = Ph, R = Cy, R = OMe and R = OPh)[33], $Na[H_2B(mp)_2]$[34] (mp = 2-mercaptopyridyl) and $Na[H_2B(mbz)_2]$[35] (mbz = 2-mercaptobenzothiazolyl), 1-ethynyl-4-nitro-benzene[36] were synthesized according to the literature procedures and other chemicals such as methyl propiolate, phenyl acetylene, diphenyl acetylene were obtained commercially (Alfa Aesar) and used as received. The external reference for the ^{11}B NMR spectroscopy, $[Bu_4N][(B_3H_8)]$ was synthesized according to the literature method.[37] The ^1H, $^{11}B\{^1H\}$, $^{13}C\{^1H\}$, $^{31}P\{^1H\}$ and HSQC NMR spectra were recorded on Bruker 400 and 500 MHz instruments. The residual solvent protons were used as reference (δ, ppm, benzene-d_6, 7.16, $CDCl_3$, 7.26), while a sealed tube containing $[Bu_4N][(B_3H_8)]$ in benzene-d_6 (δ_B, ppm, -30.07) was used as an external reference for ^{11}B NMR spectra. ^1H decoupled $^{11}B\{^1H\}$ spectra of all compounds were processed with a backward linear prediction algorithm to remove the broad $^{11}B\{^1H\}$ background signal of the NMR tube.[38] The preparative TLC was performed with Merck 105554 TLC silica gel 60 F254 and thickness of layer 250 μm on aluminum sheets with 20x20 cm size. Mass spectra were carried out using Qtof Micro YA263 HRMS instrument and Bruker MicroTOF-II mass spectrometer in ESI ionization mode. Infrared spectra were obtained on a Jasco FT/IR–1400 spectrometer. The photoreactions were carried out in a Luzchem LZC-4V photoreactor, with irradiation at 254 nm.

Synthesis of 2a-d and 3: In a flame dried Schlenk tube, [(η^6-*p*-cymene)$RuCl_2PPh_3$], **1a** (0.120 g, 0.211 mmol) and $Na[H_2B(mp)_2]$, (mp = 2-mercapto-pyridyl) (0.108 g, 0.422 mmol) were taken and placed at room temperature. Dry THF (15 mL) was slowly added to these solids under stirring condition. Upon addition of THF, a reddish orange solution formed, which was stirred at room temperature for 12 h. The volatile components were removed under vacuum and the remaining residue was dissolved in CH_2Cl_2 (15 mL)/Hexane (5 mL), passed through Celite. After removal of solvent, the residue was subjected to chromatographic workup using silica-gel TLC plates. Elution with a CH_2Cl_2/hexane (70:30 v/v) mixture yielded orange **2a** (0.063 g, 42%) and violet **3** (0.030 g, 25%).

Under similar reaction conditions, treatment of one equivalent of [(η^6-*p*-cymene)$RuCl_2PR_3$], (**1b**: R = Cy; **1c**: R = OMe; **1d**: R = OPh) with two equivalents of $Na[H_2B(mp)_2]$ yielded corresponding **2b** (0.056 g, 37%), **2c** (0.045g, 28%) and **2d** (0.042 g, 26%) along with **3** [**2b** with **3**(0.040 g, 26%), **2c** with **3** (0.052 g, 28%) and **2d** with **3** (0.046 g, 31%)].

2a: MS (ESI$^+$): *m/z* calculated for $C_{33}H_{30}BN_3PRuS_3$ $[M+H]^+$: 707.0408, found 707.0438; $^{11}B\{^1H\}$ NMR (160 MHz, $CDCl_3$, 22 °C): δ = 9.6 ppm (br, B); ^1H NMR (500 MHz, $CDCl_3$, 22 °C): δ = 8.02 (d, J = 6.3 Hz, $1H_{Ar(mp)}$), 7.50 (d, J = 6.4 Hz, $1H_{Ar(mp)}$), 7.36 (d, J = 8.6 Hz, $1H_{Ar(mp)}$), 7.31-7.22 (m, $7H_{Ar}$), 7.11 (d, J = 7.1 Hz, $2H_{Ar}$), 7.04 (t, J = 7.1 Hz, $6H_{Ar}$), 6.99 (d, J = 5.3 Hz, $2H_{Ar(mp)}$), 6.90 (t, J = 7.6 Hz, $1H_{Ar(mp)}$), 6.78-6.71 (m, $1H_{Ar(mp)}$), 6.68 (t, J = 7.6 Hz, $1H_{Ar(mp)}$), 6.52 (t, J = 6.5 Hz, $1H_{Ar(mp)}$), 6.40 (t, J = 6.5 Hz, $1H_{Ar(mp)}$), 6.16 (d, J = 8.1 Hz, $1H_{Ar(mp)}$), 6.03 (t, J = 6.3 Hz, $1H_{Ar(mp)}$), 4.05 (s, 1H, B-H_t), -14.61 ppm (s, 1H, Ru-H-B); $^{13}C\{^1H\}$ NMR (125 MHz, $CDCl_3$, 22 °C): δ = 113.0, 113.5, 114.5, 124.4, 126.2, 127.7, 129.6, 129.7, 129.8, 130.2, 130.5, 133.1, 134.1, 134.4 (Ph), 142.2, 144.3, 148.6 (C=N), 179.5, 183.2, 184.8 ppm (C=S); $^{31}P\{^1H\}$ NMR (202 MHz, $CDCl_3$, 22 °C): δ = 49.8 ppm; IR (CH_2Cl_2): $\tilde{\nu}$ = 2467 (B-H_t), 2033 cm^{-1} (B-H_b).

2b: MS (ESI$^+$): *m/z* calculated for $C_{33}H_{47}BN_3PRuS_3$ $[M]^+$: 725.1816, found 725.1807; $^{11}B\{^1H\}$ NMR (160 MHz, $CDCl_3$, 22 °C): δ = 10.1 ppm (br, B); ^1H NMR (400 MHz, $CDCl_3$, 22 °C): δ = 8.25 (d, J = 5.9 Hz, $1H_{Ar(mp)}$), 7.59 (d, J = 6.2 Hz, $1H_{Ar(mp)}$), 7.51 (d, J = 8.8 Hz, $1H_{Ar(mp)}$), 7.40 (d, J = 4.9 Hz, $1H_{Ar(mp)}$), 7.32 (d, J = 8.4 Hz, $1H_{Ar(mp)}$), 7.04-6.93 (m, $3H_{Ar(mp)}$), 6.83 (dd, J = 17.4, 10.2 Hz, 2H), 6.68-6.57 (m, 3H), 6.47 (t, J = 6.3 Hz, 1H), 6.31 (t, J = 6.0 Hz, 1H), 4.54 (s, 1H,B-H_t), 1.90 (d, J = 51.8 Hz, $10H_{Cy}$), 1.74-1.44 (m, $14H_{Cy}$), 1.38-1.22 (m, $9H_{Cy}$), -15.17 ppm (s, 1H, Ru-*H*-B); $^{13}C\{^1H\}$ NMR (125 MHz, $CDCl_3$, 22 °C): δ = 26.9 (Cy), 27.8 (Cy), 27.9 (Cy), 28.1 (Cy), 28.2, 35.7 (Cy), 35.9 (Cy), 113.7, 114.3, 115.2,126.6, 130.5, 131.1, 133.1, 133.8 (Ph), 143.5, 145.6 (C=N), 150.7 ppm; $^{31}P\{^1H\}$ NMR (202 MHz, $CDCl_3$, 22 °C): δ = 43.2 ppm; IR (CH_2Cl_2,): $\tilde{\nu}$ = 2435 (B-H_t), 2017 cm^{-1} (B-H_b).

2c: MS (ESI$^+$): *m/z* calculated for $C_{18}H_{24}BN_3O_3PRuS_3$ $[M+H]^+$: 569.9857, found 569.9814; $^{11}B\{^1H\}$ NMR (160 MHz, $CDCl_3$, 22 °C): δ = 7.7 ppm (br, B); ^1H NMR (500 MHz, $CDCl_3$, 22 °C): δ = 8.14 (d, J = 5.5 Hz, $1H_{Ar(mp)}$), 7.87 (d, J = 6.5 Hz, $2H_{Ar(mp)}$), 7.59 (d, J = 8.6 Hz, $1H_{Ar(mp)}$), 7.53 (d, J = 8.5 Hz, $1H_{Ar(mp)}$), 7.22 (d, J = 1.7 Hz, $1H_{Ar(mp)}$), 7.07 (t, J = 8.2 Hz, $1H_{Ar(mp)}$), 7.01 (dd, J = 8.8, 6.6 Hz, $1H_{Ar(mp)}$), 6.70 (d, J = 8.3 Hz, $1H_{Ar(mp)}$), 6.66 – 6.53 (m, $3H_{Ar(mp)}$), 4.37 (s, 1H, B-H_t), 3.47 (d, J = 11.0 Hz, 9H, $P(OCH_3)_3$), -15.48 ppm (s, 1H, Ru-*H*-B); $^{31}P\{^1H\}$ NMR (202 MHz, $CDCl_3$, 22 °C): δ = 146.2; IR (CH_2Cl_2): $\tilde{\nu}$ = 2496 (B-H_t), 2119 cm^{-1} (B-H_b).

2d: MS (ESI$^+$): *m/z* calculated for $C_{33}H_{30}RuS_3N_3BPO_3$ $[M+H]^+$: 756.0334, found 756.0264; $^{11}B\{^1H\}$ NMR (160 MHz, $CDCl_3$, 22 °C): δ = 7.8 ppm (br, B); ^1H NMR (500 MHz, $CDCl_3$, 22 °C): δ = 7.77 (d, J = 6.1 Hz, $1H_{Ar(mp)}$), 7.62 (d, J = 6.7 Hz, $1H_{Ar(mp)}$), 7.53 – 7.49 (m, $2H_{Ar(mp)}$), 7.43 (d, J = 5.4 Hz, $1H_{Ar(mp)}$), 7.13 (t, J = 7.8 Hz, $5H_{Ar}$), 7.07 (m, $5H_{Ar}$), 7.02 (d, J = 7.8 Hz, $3H_{Ar}$), 6.97 (m, $3H_{Ar}$), 6.62 – 6.55 (m, $4H_{Ar(mp)}$), 6.17 – 6.13 (m, $1H_{Ar(mp)}$)., 3.60 (s, 1H, B-H_t), -15.19 ppm (s, 1H, Ru-*H*-B); $^{13}C\{^1H\}$ NMR (125 MHz, $CDCl_3$, 22 °C): δ = 114.2, 120.6, 120.7, 123.6, 126.1, 133.2, 133.2, 144.2, 145.1, 148.9 ppm; $^{31}P\{^1H\}$ NMR (202 MHz, $CDCl_3$, 22 °C): δ = 128.7 ppm; IR (CH_2Cl_2): $\tilde{\nu}$ = 2454 (B-H_t), 2195 cm^{-1} (B-H_b).

3: MS (ESI$^+$): *m/z* calculated for $C_{20}H_{21}B_2N_4RuS_4$ $[M+H]^+$: 568.9888, found 568.9781; $^{11}B\{^1H\}$ NMR (160 MHz, $CDCl_3$, 22 °C): 8.5 ppm (s, B); ^1H NMR (500 MHz, $CDCl_3$, 22 °C): δ = 8.08 (d, J = 6.0 Hz, $1H_{Ar(mp)}$), 7.82 (d, J = 6.1 Hz, $1H_{Ar(mp)}$), 7.57 (t, J = 8.1 Hz, $5H_{Ar(mp)}$), 7.22 (dd, J = 16.5, 9.4 Hz, $6H_{Ar(mp)}$), 6.87 (dd, J = 13.2, 6.5 Hz, $1H_{Ar(mp)}$), 6.76 (t, J = 7.7 Hz, $1H_{Ar(mp)}$), 6.06 (d, J = 8.1 Hz, $1H_{Ar(mp)}$), 4.59 (s, 2H, B-H_t), -5.15 ppm (s, 2H, Ru-*H*-B); $^{13}C\{^1H\}$ NMR (125 MHz, $CDCl_3$, 22 °C): δ = 113.8, 126.3, 126.4, 127.9, 131.4, 133.0 (Ph), 144.5, 146.4 (C=N), 177.0 ppm (C=S); IR (CH_2Cl_2): $\tilde{\nu}$ = 2461 (B-H_t), 2056 cm^{-1} (B-H_b).

Synthesis of 2a' and 2b': Complex [(η^6-*p*-cymene)$RuCl_2PPh_3$], **1a** (0.120 g, 0.211 mmol) and $Na[H_2B(mbz)_2]$ (mbz = 2-mercaptobenzothiazolyl) (0.155 g, 0.422 mmol) were taken in a flamed dried Schlenk flask and placed at room temperature. Dry THF (15 mL) was slowly added to these solids under stirring condition, which was further stirred at room temperature for 12 h. The volatile components were removed under vacuum and the remaining reddish orange residue was dissolved in CH_2Cl_2 (15 mL)/Hexane (5 mL), passed through Celite. After removal of solvent, the residue was subjected to chromatographic workup using silica-gel TLC plates. Elution with a CH_2Cl_2/hexane (70:30 v/v) mixture yielded brown **2a'** (0.056 g, 30%) and yellow **3'** (0.060 g, 36%).

Under similar reaction conditions, reaction of [(η^6-p-cymene)$RuCl_2PCy_3$], **1b** (0.120 g, 0.206 mmol) with $Na[H_2B(mbz)_2]$ (0.152 g, 0.413 mmol) yielded red **2b'** (0.065 g, 35%) and yellow **3'** (0.043 g, 27%).

2a': MS (ESI$^+$): *m/z* calculated for $C_{39}H_{29}BN_3PRuS_6$ $[M]^+$: 874.9570, found 874.9587; $^{11}B\{^1H\}$ NMR (160 MHz, $CDCl_3$, 22 °C): δ = -3.4 ppm (br, B); ^1H NMR (400 MHz, $CDCl_3$, 22 °C): δ = 7.97 (d, J = 8.5 Hz, $1H_{Ar(mbz)}$), 7.73 (dd, J = 13.4, 7.6 Hz, $3H_{Ar(mbz)}$), 7.49 (m, $10H_{Ar}$), 7.35 (d, J = 6.9 Hz, $3H_{Ar(mbz)}$), 7.22 (d, J = 7.3 Hz, $3H_{Ar(mbz)}$), 7.12 (t, J = 7.8 Hz, $5H_{Ar}$), 6.99 (t, J = 7.3 Hz, $1H_{Ar(mbz)}$), 6.92 (t, J = 7.4 Hz, $1H_{Ar(mbz)}$), 4.98 (s, 1H, B-H_t), -3.68 ppm (s, 1H, Ru-*H*-B); $^{13}C\{^1H\}$ NMR (125 MHz, $CDCl_3$, 22 °C): δ = 115.9, 116.5, 116.7, 120.7, 120.9, 121.3, 122.2, 123.9, 124.3, 125.4, 126.3, 126.5, 127.7, 127.7, 128.6, 128.6, 129.5, 131.7, 132.0, 132.2, 132.3, 132.4, 132.9, 133.3, 134.0, 134.1, 145.6(C-N), 150.9, 167.4, 179.4 ppm (C=S); $^{31}P\{^1H\}$ NMR (202 MHz, $CDCl_3$, 22 °C): δ = 63.9 ppm; IR (CH_2Cl_2): $\tilde{\nu}$ = 2458 (B-H_t), 2043 cm^{-1} (B-H_b).

2b': MS (ESI$^+$): *m/z* calculated for $C_{39}H_{47}BN_3PRuS_6$ $[M]^+$: 893.0979, found 893.0930; $^{11}B\{^1H\}$ NMR (160 MHz, $CDCl_3$, 22 °C): δ = -3.7 ppm (br, B); ^1H NMR (400 MHz, $CDCl_3$, 22 °C): δ = 7.72 (d, J = 8.3 Hz, $1H_{Ar(mbz)}$), 7.56 (d, J = 7.9 Hz, $1H_{Ar(mbz)}$), 7.47 – 7.45 (m, $2H_{Ar(mbz)}$), 7.34 – 7.29 (m, $2H_{Ar(mbz)}$), 7.22 (d, J = 7.8 Hz, $1H_{Ar(mbz)}$), 7.14 – 7.09 (m, $3H_{Ar(mbz)}$), 6.97 (d, J = 7.3 Hz, $2H_{Ar(mbz)}$), 4.51 (s, 1H, B-H_t), 2.35 (m, H_{Cy}), 2.33 (s, $6H_{Cy}$), 1.54 – 0.84 (m, $14H_{Cy}$), -4.78 ppm (br, s, 1H, Ru-*H*-B); $^{13}C\{^1H\}$ NMR (125 MHz, $CDCl_3$, 22 °C): δ = 26.6 (Cy), 28.0 (Cy), 29.3 (Cy), 36.7(Cy), 115.8, 116.2, 116.8, 118.3, 120.8, 120.9, 121.0, 122.4, 123.7, 124.0, 125.4, 126.1, 126.2, 126.4, 131.8, 132.0, 132.2, 145.4, 145.7 (C=N), 165.3, 176.2 ppm (C=S); $^{31}P\{^1H\}$ NMR (202 MHz, $CDCl_3$, 22 °C): δ = 57.9 ppm; IR (CH_2Cl_2): $\tilde{\nu}$ = 2437 (B-H_t), 2028 cm^{-1} (B-H_b).

Note that under similar reaction conditions, compounds **2c'** and **2d'** have been synthesized along with **3'**.[19d]

Synthesis of 4 and 5: In a flame dried Schlenk tube, a brown solution of **2a'** (0.100 g, 0.11 mmol) and methyl propiolate (0.11 mL, 0.11 mmol) in toluene (15 mL) was thermalized for 12 h at 60 °C temperature. The volatile components were removed under vacuum and the remaining residue was extracted into CH_2Cl_2/hexane and passed through Celite. After removal of solvent, the residue was subjected to chromatographic work up using prepared glass TLC plates. Elution with a hexane/CH_2Cl_2 (10:90 v/v) yielded purple **4** (0.046 g, 42%) and yellow **5** (0.025 g, 22%). Note that **4** (0.060g, 54%) and **5** (0.020g, 18%) also formed when a reaction of a brown solution of **2a'** (0.050 g, 0.057 mmol) and methyl propiolate (0.05 mL, 0.057 mmol) in toluene (15 mL) was irradiated at 254 nm for 6 h at room temperature. Also, note that the yield of **5** significantly improved (0.064g, 58%) on heating **4** at 90 °C in toluene for 12h.

4: MS (ESI$^+$): *m/z* calculated for $C_{43}H_{34}BN_3PO_2RuS_6$ $[M+H]^+$: 959.9861, found 959.9872; $^{11}B\{^1H\}$ NMR (160 MHz, $CDCl_3$, 22 °C): δ = -4.8 ppm (br, B;) ^1H NMR (500 MHz, $CDCl_3$, 22 °C): δ = 8.04 (d, J = 8.3 Hz, $1H_{Ar(mbz)}$), 7.39 (dd, J = 15.0, 6.8 Hz, $4H_{Ar(mbz)}$), 7.33 – 7.27 (m, $7H_{Ar}$), 7.20 – 7.15 (m, $8H_{Ar}$), 7.10 – 7.05 (m, $6H_{Ar(mbz)}$), 7.04 – 6.98 (m, $1H_{Ar(mbz)}$), 6.72 (d, J = 13.4 Hz, 1H, *CH*COOCH$_3$), 4.32 (br, 1H, B-H_t), 3.32 (s, 3H, OCH_3), -6.70 ppm (br, 1H, Ru-*H*-B); $^{13}C\{^1H\}$ NMR (125 MHz, $CDCl_3$, 22 °C): δ = 50.6 (OCH_3), 115.2, 115.7, 116.7, 121.1, 121.6 (C=C), 124.0, 124.4, 126.2, 127.6, 129.1, 132.4, 133.8, 139.2, 145.6 (C=N); $^{31}P\{^1H\}$ NMR (202 MHz, $CDCl_3$, 22 °C): δ = 51.9 ppm; IR (CH_2Cl,): $\tilde{\nu}$ = 2454 (B-H_t), 1952 (B-H_b), 1686 (CO), 1585 cm^{-1} (C=C).

5: MS (ESI$^+$): *m/z* calculated for $C_{43}H_{34}BN_3PO_2RuS_6$ $[M+H]^+$: 959.9861, found 959.9872; $^{11}B\{^1H\}$ NMR (160 MHz, $CDCl_3$, 22 °C): δ = -4.3 ppm (br, B); ^1H NMR (500 MHz, $CDCl_3$, 22 °C): δ = 8.14 (d, J = 8.4 Hz, $1H_{Ar(mbz)}$), 7.45 – 7.34 (m, $4H_{Ar}$), 7.28 (d, J = 7.5 Hz, $1H_{Ar(mbz)}$), 7.22 (d, J = 7.8 Hz, $2H_{Ar(mbz)}$), 7.20 – 7.13 (m, $6H_{Ar}$), 7.06-7.00 (m, $5H_{Ar}$), 6.97 (d, J = 6.9 Hz, $6H_{Ar(mbz)}$), 6.76 (t, J = 7.5 Hz, $1H_{Ar(mbz)}$), 6.69 (t, J = 7.6 Hz, $1H_{Ar(mbz)}$), 6.42 (s, 1H, *CH*COOCH$_3$), 5.16 (br, 1H, B-H_t), 3.58 (s, 3H, *OCH$_3$*), -5.89 ppm (s, 1H, Ru-*H*-B); $^{13}C\{^1H\}$ NMR (125 MHz, $CDCl_3$, 22 °C): δ = 50.5 (OCH_3), 115.5, 116.3, 119.6, 121.2 (C=CH), 121.9, 123.9, 124.3, 125.4, 126.2, 127.5, 128.9, 133.3, 133.9, 134.3 (C=C), 145.3, 145.6 (C=N),

149.7 (C=N), 164.5 (C=S), 175.4 (CO), 195.9, 198.5 ppm (C=S); $^{31}P\{^{1}H\}$ NMR (202 MHz, $CDCl_3$, 22 °C): δ = 48.8 ppm; IR (CH_2Cl_2): $\tilde{\nu}$ = 2445 (B-H_t), 1956 (B-H_b), 1662 (CO), 1532 cm^{-1} (C=C).

Synthesis of 4' and 5': Compounds **4'** and **5'** were synthesized from the reaction of **2a'** (0.100 g, 0.11 mmol) with 1-ethynyl-4-nitrobenzene (0.017 g, 0.11 mmol) under the same thermolytic [**4'** (0.030 g, 25%) and **5'** (0.074 g, 63%)] as well as photolytic [**4'** (0.065 g, 55%) and **5'** (0.018 g, 15%)] reaction conditions as needed for compounds **4** and **5**.

4': MS (ESI^+): *m/z* calculated for $C_{47}H_{35}BN_4PO_2RuS_6$ $[M+H]^+$: 1022.9972, found 1022.9993; $^{11}B\{^{1}H\}$ NMR (160 MHz, $CDCl_3$, 22 °C): δ = -5.2 ppm (br, B); ^{1}H NMR (400 MHz, $CDCl_3$, 22 °C): δ = 8.29 (d, *J* = 8.5 Hz, 1H $_{Ar(mbz)}$), 8.08 (d, *J* = 9.2 Hz, 2H $_{Ar(mbz)}$), 7.77 (d, *J* = 9.5 Hz, 5H $_{Ar}$), 7.71 (dd, *J* = 11.8, 6.6 Hz, 2H $_{Ar}$), 7.55 – 7.40 (m, 3H $_{Ar}$), 7.34 (t, *J* = 8.7 Hz, 6H $_{Ar(mbz)}$), 7.23 – 7.13 (m, 4H $_{Ar(mbz)}$), 7.06 (d, *J* = 8.0 Hz, 6H $_{Ar(mbz)}$), 6.87 (dd, *J* = 32.8, 8.4 Hz, 3H $_{Ar(mbz)}$), 6.77 (s, 1H *C=CH*), 4.49 (s, 1H, B-*H*$_t$), -7.04 ppm (br, 1H, Ru-*H*-B); $^{31}P\{^{1}H\}$ NMR (202 MHz, $CDCl_3$, 22 °C): δ = 52.2 ppm; IR (CH_2Cl_2): $\tilde{\nu}$ = 2431 (B-H_t), 2020 cm^{-1} (B-H_b).

5': MS (ESI^+): *m/z* calculated for $C_{47}H_{35}BN_4PO_2RuS_6$ $[M+H]^+$: 1022.9972, found 1022.9993; $^{11}B\{^{1}H\}$ NMR (160 MHz, $CDCl_3$, 22 °C): δ = -4.5 ppm (br, B;) ^{1}H NMR (500 MHz, $CDCl_3$, 22 °C): δ = 8.28 – 8.24 (m, 2H $_{Ar(mbz)}$), 8.10 (d, *J* = 7.9 Hz, 2H $_{Ar(mbz)}$), 7.70 (d, *J* = 7.1 Hz, 2H $_{Ar(mbz)}$), 7.62 – 7.44 (m, 5H $_{Ar}$), 7.38 (d, *J* = 7.6 Hz, 1H $_{Ar(mbz)}$), 7.29 – 7.26 (m, 7H $_{Ar(mbz)}$), 7.16 – 7.05 (m, 10H $_{Ar}$), 6.89 – 6.76(m, 3H $_{Ar(mbz)}$), 4.65 (s, 1H, B-*H*$_t$), -6.16 ppm (br, 1H, Ru-*H*-B); $^{13}C\{^{1}H\}$ NMR (125 MHz, $CDCl_3$, 22 °C): δ = 113.4, 115.5, 116.3, 121.1(C=C), 123.8, 124.5, 125.6, 133.3, 134.7, 145.3, 145.7, 147.9, 149.7, 173.0, 189.6(C=S), 196.0 ppm (C=S); $^{31}P\{^{1}H\}$ NMR (202 MHz, $CDCl_3$, 22 °C): δ = 50.8 ppm; IR (CH_2Cl_2): $\tilde{\nu}$ = 2424 (B-H_t), 2028 cm^{-1} (B-H_b).

Synthesis of 6 and 7: Under similar reaction conditions, compounds **6** (0.034 g, 31%) and **7** (0.024 g, 21%) were isolated from the reaction of **2b'** and **2c'** respectively with methyl propiolate.

6: HRMS (ESI^+): *m/z* calculated for $C_{43}H_{51}RuS_6N_3B_1PO_2$ $[M]^+$: 977.1192, found 977.1147; $^{11}B\{^{1}H\}$ NMR (160 MHz, $CDCl_3$, 22 °C): δ = -4.6 ppm (br, B); ^{1}H NMR (500 MHz, $CDCl_3$, 22 °C): δ = 8.33 (d, *J* = 8.4 Hz, 1H$_{Ar(mbz)}$), 7.84 (d, *J* = 8.3 Hz, 1H$_{Ar(mbz)}$), 7.58 (t, *J* = 7.8 Hz, 1H$_{Ar(mbz)}$), 7.51 (d, *J* = 7.9 Hz, 1H$_{Ar(mbz)}$), 7.34 – 7.33 (m, 2H$_{Ar(mbz)}$), 7.23 – 7.13 (m, 2H$_{Ar(mbz)}$), 7.09 (t, *J* = 7.5 Hz, 1H$_{Ar(mbz)}$), 7.04 (t, *J* = 7.5 Hz, 1H$_{Ar(mbz)}$), 6.98 (t, *J* = 7.5 Hz, 2H$_{Ar(mbz)}$), 6.91 (s, 1H, C*H*COOCH$_3$), 5.26 (s, 1H, B-*H*$_t$), 3.72 (s, 3H, *OCH*$_3$), 1.75 (dt, *J* = 26.0, 12.7 Hz, 5H$_{Cy}$), 1.72 – 1.63 (m, 5H$_{Cy}$), 1.52 (s, 15H$_{Cy}$), 1.08 – 0.94 (m, 8H$_{Cy}$), -6.05 ppm (br, 1H, Ru-*H*-B); $^{13}C\{^{1}H\}$ NMR (125 MHz, $CDCl_3$, 22 °C): δ = 26.9, 28.0, 28.0, 29.8, 50.5 (O*CH*$_3$), 115.2, 116.2, 118.6, 120.9 (C=CH), 121.6, 121.7, 122.6, 123.6, 124.1, 124.3, 125.4, 126.2, 126.4, 134.0 (C=C), 145.8 (C=N), 150.7 (C=N), 164.4 (C=S), 176.3 (CO), 195.7 (C=S); $^{31}P\{^{1}H\}$ NMR (202 MHz, $CDCl_3$, 22 °C): δ = 38.0 ppm; IR (CH_2Cl_2): $\tilde{\nu}$ = 2414 (B-H_t), 1948 (B-H_b), 1640 (CO), 1495 cm^{-1} (C=C).

7: MS (ESI^+): *m/z* calculated for $C_{28}H_{28}BN_3PO_5RuS_6$ $[M+H]^+$: 821.9233, found 821.9220; $^{11}B\{^{1}H\}$ NMR (160 MHz, $CDCl_3$, 22 °C): δ = -5.4 ppm (br, B); ^{1}H NMR (400 MHz, $CDCl_3$, 22 °C): δ = 8.19 (d, *J* = 8.5 Hz, 1H$_{Ar(mbz)}$), 7.79 – 7.77 (m, 1H$_{Ar(mbz)}$), 7.52 (dd, *J* = 7.2, 3.2 Hz, 2H$_{Ar(mbz)}$), 7.38 (d, *J* = 7.8 Hz, 1H$_{Ar(mbz)}$), 7.34 (d, *J* = 8.3 Hz, 1H$_{Ar(mbz)}$), 7.20 (d, *J* = 4.3 Hz, 2H $_{Ar(mbz)}$), 7.11 (dt, *J* = 23.4, 7.5 Hz, 2H$_{Ar(mbz)}$), 7.01 (dd, *J* = 6.6, 3.0 Hz, 2H$_{Ar(mbz)}$), 6.76 (s, 1H, *CH*COOCH$_3$), 4.81 (s, 1H, B-*H*$_t$), 3.74 (s, 3H, *OCH*$_3$), 3.39 (d, *J* = 10.9 Hz, 9H, *P(OCH*$_3$*)*$_3$), -6.48 ppm (s, 1H, Ru-*H*-B); $^{31}P\{^{1}H\}$ NMR (202 MHz, $CDCl_3$, 22 °C): δ = 144.3 ppm; IR (CH_2Cl_2): $\tilde{\nu}$ = 2425 (B-H_t), 1954 (B-H_b), 1729 (CO), 1653 cm^{-1} (C=C).

Computational details: All molecules were fully optimized with the Gaussian 09[39] program using the BP86[40] functional in conjunction with def2-SVP[41] basis set from EMSL[42] Basis Set Exchange Library. The 28 core electrons of ruthenium was replaced by quasi-relativistic def2-ECP effective core potentials.[43] The X-ray crystallographic coordinates were used for geometry optimizations in gaseous state (no solvent effect). The frequency calculations were carried out at the same level of theory using the optimized coordinates and the absence of any imaginary frequencies confirmed that all structures represent minima on the potential energy hypersurface. We have computed ^{11}B and ^{1}H NMR chemical shifts using gauge-including atomic orbitals (GIAOs)[44] method at the same level. The ^{11}B NMR chemical shifts were calculated relative to B_2H_6 and converted to the usual [BF_3.OEt_2] scale[45] and ^{1}H NMR calculations TMS ($SiMe_4$) was used as internal standard. Natural bonding analyses were carried out with the natural bond orbital (NBO) 6.0 version of program.[46] Wiberg bond indices (WBI)[47] were obtained on natural bond orbital analysis. In order to understand the nature of bonding of the synthesised molecules in detail, the topological parameters were obtained from the wave functions of all the optimized structures, were analysed with the quantum theory of atoms in molecules (QTAIM).[48] The QTAIM analysis was carried out utilizing Multiwfn Version 3.6 package.[49]

X-ray Structure Determination analysis details: Single crystals of **2a**, **2b**, and **2a'** were obtained from slow diffusion of a hexane-CH_2Cl_2 solution, while **4**, **5** and **5'** were grown by slow diffusion of a toluene-CH_2Cl_2 solution. Crystal data of **2a**, **4**, **5** and **5'** were obtained using D8 VENTURE Bruker AXS diffractometer, with multilayer monochromated $Mo_{K\alpha}$ (λ = 0.71073 Å) radiation at 150(2) K. Crystal data of **2a'** was obtained using a Bruker AXS Kappa APEXII CCD diffractometer with graphite monochromated Mo-Kα (λ = 0.71073 Å) radiation at 296(2) K and crystal data of **2b** was obtained by OXFORD DIFFRACTION SUPER NOVA with multilayer monochromated $Mo_{K\alpha}$ (λ = 0.71073 Å) radiation at 298(2) K. The structures were solved by direct methods using SIR97[50] and refined using SHELXL-2014 or SHELXL-2016[51]. The molecular structures were drawn using Olex2.[52] The non-hydrogen atoms were refined with anisotropic displacement parameters. All hydrogens could be located in the difference Fourier map. However, the hydrogen atoms bonded to carbons and borons were fixed at chemically meaningful positions and were allowed to ride with the parent atom during the refinement. These data can be obtained free of charge from The Cambridge Crystallographic Data Centre via www.ccdc.cam.ac.uk/data_request/cif.

Crystal data for 2a: CCDC 1824573, $C_{33}H_{29}BN_3PRuS_3$, M_r = 706.62, Monoclinic, space group *P2*$_1$*/n*, *a* = 9.4795(9) Å, *b* = 19.546(2) Å, *c* = 19.113(2) Å, α = 90°, β = 93.732(4)°, γ = 90°, *V* = 3533.9(7) Å^3, *Z* = 4, ρ_{calcd}= 1.328 g/cm^3, μ = 0.922 mm^{-1}, *F(000)* = 1440, R_1 = 0.0349, wR_2 = 0.0893, 8086 independent reflections [2θ ≤ 50.48°] and 385 parameters.

Crystal data for 2b: CCDC 1824574, $C_{66}H_{92}B_2N_6P_2Ru_2S_6$, M_r = 1447.51, Triclinic, space group *P-1*, *a* = 10.065(2) Å, *b* = 19.412(4) Å, *c* = 21.860(4) Å, α = 109.26(3)°, β = 98.20(3)°, γ = 104.77(3)°, *V* = 3776.8(16) Å^3, *Z* = 2, ρ_{calcd}= 1.273 g/cm^3, μ = 0.648 mm^{-1}, *F(000)* = 1508, R_1 = 0.0731, wR_2 = 0.2055, 13251 independent reflections [2θ ≤ 49.66°] and 757 parameters.

Crystal data for 2a': CCDC 1824572, $C_{40}H_{31}BCl_2N_3PRuS_6$, M_r = 959.79, Monoclinic, space group *P2*$_1$*/c*, *a* = 19.537(6) Å, *b* = 8.483(2) Å, *c* = 25.650(8) Å, α = 90°, β = 108.784(9)°, γ = 90°, *V* = 4025(2) Å^3, *Z* = 4, ρ_{calcd} = 1.584 g/cm^3, μ = 0.909 mm^{-1}, *F(000)* = 1944, R_1 = 0.0449, wR_2 = 0.0883, 6411 independent reflections [2θ ≤ 49.5°] and 552 parameters.

Crystal data for 4: CCDC 1588860, $C_{50}H_{41}BN_3O_2PRuS_6$, M_r = 1051.07, Triclinic, space group *P-1*, *a* = 11.0668(14) Å, *b* = 11.1808(16) Å, *c* =

19.716(3) Å, α = 98.269(5)°, β = 90.119(5)°, γ = 103.118(5)°, V = 2349.7(6) Å^3, Z = 2, ρ_{calcd}= 1.486 g/cm^3, μ = 0.679 mm^{-1}, *F(000)* = 1076, R_1 = 0.0443, wR_2 = 0.1250, 10752 independent reflections [2θ ≤ 50.48°] and 585 parameters.

Crystal data for 5: CCDC 1588861, $C_{43}H_{33}BN_3O_2PRuS_6$, M_r = 958.93, Triclinic, space group *P-1*, a = 11.4444(9) Å, b = 11.5257(10) Å, c = 15.6865(14) Å, α = 91.164(3)°, β = 101.509(3)°, γ = 98.383(3)°, V = 2003.3(3) Å^3, Z = 2, ρ_{calcd} = 1.590 g/cm^3, μ = 0.787 mm^{-1}, *F(000)* = 976, R_1 = 0.0339, wR_2 = 0.0790, 9224 independent reflections [2θ ≤ 50.48°] and 521 parameters.

Crystal data for 5': CCDC 1848233, $C_{47}H_{34}BN_4O_2PRuS_6$, M_r = 1021.99, Monoclinic, space group $P2_1/n$, a = 15.1034(14) Å, b = 18.8061(15) Å, c = 17.8599(14) Å, α = 90°, β = 98.093(3)°, γ = 90°, V = 5022.3(7) Å^3, Z = 4, ρ_{calcd}= 1.352 g/cm^3, μ = 0.633 mm^{-1}, *F(000)* = 2080, R_1 = 0.0328, wR_2 = 0.0781, 11405 independent reflections [2θ ≤ 50.48°] and 530 parameters.

Acknowledgements

This work was supported by CEFIPRA (grant number 5905-1), New Delhi, India. MZ and KP thank IIT Madras for research fellowship. RR thanks University Grants Commission (UGC), India for fellowship. IIT Madras is gratefully acknowledged for computational facilities.

Keywords: insertion • terminal alkyne • ruthenium• borate • chelating ligand

[1] a) Transition Metals for Organic Synthesis, (Eds.: M. Beller, C. Bolm) Wiley-VCH: Weinheim, Germany, **2004**; b) J. Choi, A. H. Roy MacArthur, M. Brookhart, A. S. Goldman, *Chem. Rev.* **2011**, *111*, 1761–1779; c) S. Diez-Gonzalez, N. Marion, S. P. Nolan, *Chem. Rev.* **2009**, *109*, 3612–3676; d) B. M. Trost, M. L. Crawley, *Chem. Rev.* **2003**, *103*, 2921–2943; d) B. M. Trost, D. L. Van Vranken, *Chem. Rev.* **1996**, *96*, 395–422.

[2] a) J. R. Khusnutdinova, D. Milstein, *Angew. Chem.* **2015**, *127*, 12406–12445; *Angew. Chem. Int. Ed.* **2015**, *54*, 12236–12273; b) P. J. Chirik, K. Wieghardt, *Science*, **2010**, *327*, 794–795.

[3] a) R. Peters, *Cooperative Catalysis*, Wiley-VCH: Weinheim, **2015**; b) H. Grützmacher, *Angew. Chem.* **2008**, *120*, 1838–1842; *Angew. Chem., Int. Ed.* **2008**, *47*, 1814–1818.

[4] a) C. Gunanathan, D. Milstein, *Acc. Chem. Res.* **2011**, *44*, 588–602; b) T. Zell, D. Milstein, *Acc. Chem. Res.* **2015**, *48*, 1979–1994; c) C. Gunanathan, D. Milstein, *Chem. Rev.* **2014**, *114*, 12024–12087; d) C. Gunanathan, D. Milstein, *Top. Organomet. Chem.* **2011**, *37*, 55–84; e) D. Milstein, *Top. Catal.* **2010**, *53*, 915–923; f) E. Balaraman, C. Gunanathan, J. Zhang, L. J. W. Shimon, D. Milstein, *Nat. Chem.* **2011**, *3*, 609–614.

[5] a) D. L. Davies, S. M. A. Donald, O. Al-Duaij, S. A. Macgregor, M. Polleth, *J. Am. Chem. Soc.* **2006**, *128*, 4210–4211; b) X. Qi, Y. Li, R. Bai, Y. Lan, *Acc. Chem. Res.* **2017**, *50*, 2799–2808; c) O. Eisenstein, J. Milani, R. N. Perutz, *Chem. Rev.* **2017**, *117*, 8710–8753.

[6] a) R. H. Crabtree, *The Organometallic Chemistry of the Transition Metals*, 4th ed.; John Wiley & Sons, Inc.: Hoboken, NJ, **2005**; b) J. A. Labinger, J. E. Bercaw, *Nature* **2002**, *417*, 507–514.

[7] a) J. C. Jeffrey, T. B. Rauchfuss, *Inorg. Chem.* **1979**, *18*, 2658–2666; b) P. Braunstein, F. Naud, *Angew. Chem.* **2001**, *113*, 702–722; *Angew. Chem. Int. Ed.* **2001**, *40*, 680–699.

[8] a) D. L. J. Broere, R. Plessius, J. I. van der Vlugt, *Chem. Soc. Rev.* **2015**, *44*, 6886–6915; b) T. Tezgerevska, K. G. Alley, C. Boskovic, *Coord. Chem. Rev.* **2014**, *268*, 23–40.

[9] a) R. Noyori, *Angew. Chem.* **2002**, *114*, 2108–2123; *Angew. Chem. Int. Ed.* **2002**, *41*, 2008–2022; b) S. P. Semproni, C. Milsmann, P. J. Chirik, *J. Am. Chem. Soc.* **2014**, *136*, 9211–9224; c) B. L. Conley, M. K. Pennington-Boggio, E. Boz, T. J. Williams, *Chem. Rev.* **2010**, *110*, 2294–2312; d) D. B. Grotjahn, *Chem. Eur. J.* **2005**, *11*, 7146–7153.

[10] a) D. L. Davies, S. A. Macgregor, A. I. Poblador-Bahamonde, *Dalton Trans,* **2010**, *39*, 10520–1052; b) D. Lapointe, K. Fagnou, *Chem. Lett.* **2010**, *39*, 1119–1126; c) D. G. Johnson, J. M. Lynam, J. M. Slattery, C. E. Welby, *Dalton Trans.* **2010**, *39*, 10432–10441; d) D. Lapointe, K. Fagnou, *Chem. Lett.* **2010**, *39*, 1118–1126; e) J. Guihaume, S. Halbert, O. Eisenstein, R. N. Perutz, *Organometallics*, **2012**, *31*, 1300–1314.

[11] a) D. L. Davies, S. M. A. Donald, S. A. Macgregor, *J. Am. Chem. Soc.* **2005**, *127*, 13754–13755.

[12] M. W. Drover, J. A. Love, L. L. Schafer, *J. Am. Chem. Soc.* **2016**, *138*, 8396–8399.

[13] A. de Aguirre, S. Díez-Gonzalez, F. Maseras, M. Martín, E. Sola,´ *Organometallics* **2018**, *37*, 2645–2651.

[14] B. Breit, U. Gellrich, T. Li, J. M. Lynam, L. M. Milner, N. E. Pridmore, J. M. Slattery, A. C. Whitwood, *Dalton Trans*. **2014**, *43*, 11277–11285.

[15] a) N. M. Leeb, M. W. Drover, J. A. Love, L. L. Schafer, J. M. Slattery, *Organometallics* **2018**, *37*, 4630–4638; b) S. Oldenhof, M. Lutz, J. I. van der Vlugt, J. N. H. Reek, *Chem. Commun*. **2015**, *51*, 15200–15203.

[16] a) T. B. Marder, Z. Lin, *Contemporary Metal Boron Chemistry I. Borylenes, Boryls, Borane σ-complexes, and Borohydrides,* Springer, Berlin, 2008; b) H. Braunschweig, R. D. Dewhurst, V. H. Gessner, *Chem. Soc. Rev.* 2013, **42**, 3197–3208;

[17] a) R. S. Anju, D. K. Roy, B. Mondal, K. Yuvaraj, C. Arivazhagan, K. Saha, B. Varghese, S. Ghosh, *Angew. Chem. Int. Ed.* **2014**, *53*, 2873–2877; b) D. K. Roy, B. Mondal, R. S. Anju, S. Ghosh, *Chem. Eur. J.* **2015**, *21*, 3640–3648; c) K. Bakthavachalam, K. Yuvaraj, M. Zafar, S. Ghosh, *Chem. Eur. J.* **2016**, 22, 17291–17297; d) S. Gomosta, R. Ramalakshmi, C. Arivazhagan, A. Haridas, B. Raghavendra, K. Maheswari, T. Roisnel, S. Ghosh, *Z. Anorg. Allg. Chem.* **2019**, *645*, 588–594.

[18] a) D. K. Roy, R. Borthakur, S. Bhattacharyya, V. Ramkumar, S. Ghosh, *J. Organomet. Chem.* **2015**, *799–800*, 132–140; b) R. Ramalakshmi, K. Saha, D. K. Roy, B. Varghese, A. K. Phukan, S. Ghosh, *Chem. Eur. J.* **2015**, *21*, 17191–17195; c) K. Saha, R. Ramalakshmi, S. Gomosta, K. Pathak, V. Dorcet, T. Roisnel, J.-F. Halet, S. Ghosh, *Chem. Eur. J.* **2017**, *23*, 9812–9820; d) R. Ramalakshmi, K. Maheswari, D. Sharmila, A. Paul, T. Roisnel, J.-F. Halet, S. Ghosh, *Dalton Trans.* **2016**, *45*, 16317–16324.

[19] a) D. K. Roy, K. Yuvaraj, R. Jagan, S. Ghosh, *J. Organomet. Chem.* **2016**, *811*, 8–13; b) K. Saha, B. Joseph, R. Ramalakshmi, R. S. Anju, B. Varghese, S. Ghosh, *Chem. Eur. J.* **2016**, *22*, 7871–7878; c) K. Saha, B. Joseph, R. Borthakur, R. Ramalakshmi, T. Roisnel, S. Ghosh, *Polyhedron*, **2017**, *125*, 246–252; d) M. Zafar, R. Ramalakshmi, A. N. Pradhan, K. Pathak, T. Roisnel, J.-F. Halet, S. Ghosh, *Dalton Trans.* **2019**, *DOI: 10.1039/C9DT00498J*.

[20] a) V. P. Anju, S. K. Barik, B. Mondal, V. Ramkumar, S. Ghosh, *ChemPlusChem*, **2014**, *79*, 546-551; b) K. Geetharani, S. Tussupbayev, J. Borowka, M. C. Holthausen, S. Ghosh, *Chem. Eur. J.* **2012**, *18*, 8482–8489.

[21] D. K. Roy, P. Shankhari, K. Yuvaraj, B. Mondal, A. Sikder, S. Ghosh, *Chem. Eur. J.* **2013**, *19*, 2337–2343.

[22] R. S. Anju, B. Mondal, K. Saha, S. Panja, B. Varghese, S. Ghosh, *Chem. Eur. J.* **2015**, *21*, 11393–11400.

[23] D. J. Harding, H. Adams, T. Tuntulani, *Acta Cryst.* **2005**, *C61*, m301–m303.

[24] In parallel to the formation of **2a-d**, reactions of **1a-d** with Na[$H_2B(mp)_2$] (mp = 2-mercaptopyridyl) also yielded ruthenium bis-borate complex, [Ru{κ^3-H,S,S'-$H_2B(L)_2$}$_2$], **3** (L = C_5H_4NS), which has been characterized

by ^{1}H, ^{11}B{^{1}H}, ^{13}C{^{1}H} and IR spectroscopy. The mass spectrometry and other spectroscopic studies suggest that **3** is analogous to **3'**[19d]. The ^{11}B{^{1}H} NMR spectrum of **3** reveals a sharp signal at δ = 8.5 ppm; shifted downfield as compared to **3'** (δ = -4.8 ppm). The ^{1}H NMR spectrum of **3** displayed an upfield resonance at δ = -5.15 ppm due to the R-H-B proton. Further, the mass spectrometry provided a molecular ion peak at *m/z* 568.9781, consistent with formula of $C_{20}H_{21}B_2N_4RuS_4$.

[25] The ^{11}B{^{1}H} NMR spectra of **2a'**-**b'** show a sharp peak in the upfield region (**2a'**: δ = -3.4 ppm; **2b'**: -3.7 ppm). The ^{31}P{^{1}H} NMR spectra display a singlet at δ = 63.9 ppm for **2a'** and at δ = 57.9 ppm for **2b'**; the signals are slightly upfield-shifted as compared to those for **2c'** and **2d'**.[19d] This may be due to the fact that the π accepting ability of phosphine is more than phosphite. The ^{1}H NMR spectra display multiplets corresponding to mbz protons in the region of δ = 6.86 – 7.98 ppm and one upfield chemical shift due to Ru-H-B protons at δ = -3.77 ppm for **2a'** and δ = -4.78 ppm for **2b'**, which are shifted upfield in comparison to **2c'** (δ = -2.32 ppm) and **2d'** (δ = -2.44 ppm)[19d].

[26] S. O.Pinheiro, J. R. de Sousa, M. O. Santiago, I. M. M.Carvalho, A. L. R. Silva, A. A. Batista, E. E. Castellano, J. Ellena Í. S.Moreira, I. C. N. Diógenes, *Inorg. Chem. Acta* **2006**, *359*, 391–400.

[27] R. Mitra, A. G. Samuelson, *Eur. J. Inorg. Chem*. **2014**, 3536–3546.

[28] a) L. Omann, C. David, F. Königs, H. F. T. Klare, M. Oestreich, *Acc. Chem. Res.* **2017**, *50*, 1258–1269; b) G. A. Dide Verhoeven, M.-E. Moret, *Dalton Trans*. **2016**, *45*, 15762–15778.

[29] a) F. E. Fernández, M. C. Puerta, P. Valerga, *Inorg. Chem.* **2013**, *52*, 502–6509; b) A. García-Fernández, S. Miguel, J. Díez, M. P. Gamasa, E. Lastra, *Eur. J. Inorg. Chem.* **2016**, 2516–2526.

[30] L. Huang, M. Arndt, K. Gooßen, H. Heydt, L. J. Gooßen, *Chem. Rev.* **2015**, *115*, 2596–2697.

[31] a) M. Patel, R. K. Saunthwal, A. K. Verma, *Acc. Chem. Res.* **2017**, *50*, 240–254; b) S. W. M. Crossley, C. Obradors, R. M. Martinez, R. A. Shenvi, *Chem. Rev.* **2016**, *116*, 8912–9000; c) M. Mellah, A. Voituriez, E. Schulz, *Chem. Rev.* **2007**, *107*, 5133–5209.

[32] a) I. Strydom, G. Guisado-Barrios, I. Fernández, D. C. Liles, E. Peris, D. I. Bezuidenhout, *Chem. Eur. J.* **2017**, *23*, 1393–1401; b) J. L. Kennemur, G. D. Kortman, K. L. Hull, *J. Am. Chem. Soc.* **2016**, *138*, 11914–11919; c) A. D. Giuseppe, R. Castarlenas, J. J. Pérez-Torrente, M. Crucianelli, V. Polo, R. Sancho, F. J. Lahoz, L. A. Oro, *J. Am. Chem. Soc.* **2012**, *134*, 8171–8183.

[33] a) R. Sáez, J. Lorenzo, M. J. Prieto, M. Font-Bardia, T. Calvet, N. Omeñaca, M. Vilaseca, V. Moreno, *J. Inorg. Biochem*. **2014**, *136*, 1–12; b) E. Solari, S. Gauthier, R. Scopelliti, K. Severin, *Organometallics* **2009**, *28*, 4519–4526; c) E. E. Joslin, C. L. McMullin, T. B. Gunnoe, T. R. Cundari, M. Sabat, W. H. Myers, *Inorg. Chem.* **2012**, *51*, 4791–4801; d) E. Tomás-Mendivil, V. Cadierno, M. I. Menéndez, R. López, *Chem. Eur. J.* **2015**, *21*, 16874–16886.

[34] G. Dyson, A. Hamilton, B. Mitchell, G. R. Owen, *Dalton Trans.* **2009**, 6120–6126.

[35] M. Imran, B. Neumann, H.-G. Stammler, U. Monkowius, M. Ertl, N. W. Mitzel, *Dalton Trans*. **2014**, *43*, 1267–1278.

[36] S. A. Sharber, R. N. Baral, F. Frausto, T. E. Haas, P. Muller, S. W. Thomas, *J. Am. Chem. Soc.* ***2017***, *139*, 5164–5174.

[37] G. E. Ryschkewitsch, K. C. Nainan, *Inorg. Synth.* **1975**, *15*, 11–15.

[38] a) J. J. Led, H. Gesmar, *Chem. Rev.* **1991**, *91*, 1413–1426; b) L. Yang, R. Simionescu, A. Lough, H. Yan, *Dyes Pigm*. **2011**, *91*, 264–267.

[39] Gaussian 09, Revision C.01, M. J. Frisch, G. W. Trucks, H. B. Schlegel, G. E. Scuseria, M. A. Robb, J. R. Cheeseman, G. Scalmani, V. Barone, B. Mennucci, G. A. Petersson, H. Nakatsuji, M. Caricato, X. Li, H. P. Hratchian, A. F. Izmaylov, J. Bloino, G. Zheng, J. L. Sonnenberg, M. Hada, M. Ehara, K. Toyota, R. Fukuda, J. Hasegawa, M. Ishida, T. Nakajima, Y. Honda, O. Kitao, H. Nakai, T. Vreven, J. A. Montgomery, Jr., J. E. Peralta, F. Ogliaro, M. Bearpark, J. J. Heyd, E. Brothers, K. N. Kudin, V. N. Staroverov, T. Keith, R. Kobayashi, J. Normand, K. Raghavachari, A. Rendell, J. C. Burant, S. S. Iyengar, J. Tomasi, M. Cossi, N. Rega, J. M. Millam, M. Klene, J. E. Knox, J. B. Cross, V. Bakken, C. Adamo, J. Jaramillo, R. Gomperts, R. E. Stratmann, O. Yazyev, A. J. Austin, R. Cammi, C. Pomelli, J. W. Ochterski, R. L. Martin, K. Morokuma, V. G. Zakrzewski, G. A. Voth, P. Salvador, J. J. Dannenberg, S. Dapprich, A. D. Daniels, O. Farkas, J. B. Foresman, J. V. Ortiz, J. Cioslowski and D. J. Fox, Gaussian, Inc., Wallingford CT, **2010**.

[40] a) H. L. Schmider, A. D. Becke, *J. Chem. Phys*. **1998**, *108*, 9624–9631; b) J. P. Perdew, *Phys. Rev. B: Condens. Matter Mater. Phys.* **1986**, *33*, 8822–8824.

[41] F. Weigend, R. Ahlrichs, *Phys. Chem. Chem. Phys.* **2005**, *7*, 3297–3305.

[42] EMSL Basis Set Exchange Library. https://bse.pnl.gov/bse/portal

[43] D. Andrae, U. Häußermann, M. Dolg, H. Stoll, H. Preuß, *Theor. Chim. Acta.* **1990**, *77*, 123–141.

[44] a) F. J. London, *J. Phys. Radium* **1937**, *8*, 397-409; b) R. Ditchfield, *Mol. Phys.* **1974**, *27*, 789–807; c) K. Wolinski, J. F. Hinton, P. Pulay, *J. Am. Chem. Soc.* **1990**, *112*, 8251–8260.

[45] T. P. Onak, H. L. Landesman, R. E. Williams, I. Shapiro, *J. Phys.Chem.* **1959**, *63*, 1533–1535.

[46] NBO Program 6.0, E. D. Glendening, J. K. Badenhoop, A. E. Reed, J. E. Carpenter, J. A. Bohmann, C. M. Morales, C. R. Landis, F. Weinhold, Theoretical Chemistry Institute, University of Wisconsin, Madison, WI, **2013**.

[47] K. Wiberg, *Tetrahedron* **1968**, *24*, 1083–1096.

[48] a) R. F. W. Bader, *Atoms in Molecules: A Quantum Theory*, Oxford University Press: Oxford, U. K. **1990**; b) R. F. W. Bader, *J. Phys. Chem. A*. **1998**, *102*, 7314-7323; c) R. F. W. Bader, *Chem. Rev.* **1991**, *91*, 893–928.

[49] T. Lu, F. Chen, *J. Comput. Chem.* **2012**, *33*, 580–592.

[50] A. Altomare, M. C. Burla, M. Camalli, G. L. Cascarano, C. Giacovazzo, A. Guagliardi, A. G. G. Moliterni, G. Polidori, R. Spagna, *J. Appl. Crystallogr.* **1999**, *32*, 115–119.

[51] a) G. M. Sheldrick, *Acta Cryst. Sect. A* **2015**, *71*, 3-8; b) G. M. Sheldrick, *Acta Cryst. Sect. C* **2015**, *71*, 3–8.

[52] O. V. Dolomanov, L. J. Bourhis, R. J. Gildea, J. A. K. Howard, H. Puschmann, *J. Appl. Cryst.* **2009**, *42*, 339–341.

10.1002/chem.201902663

WILEY-VCH

Entry for the Table of Contents

FULL PAPER

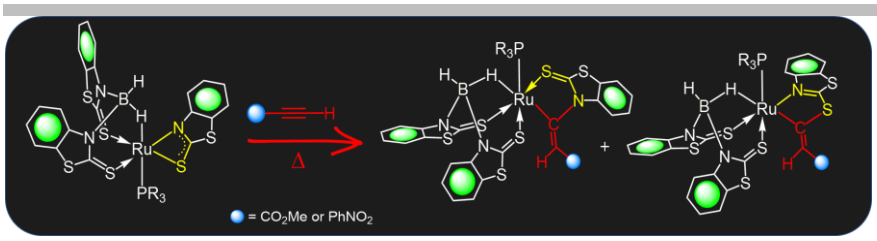

Thermolysis of ruthenium borate complexes having hemilabile *N*,*S*-chelating ligand with terminal alkynes yielded five-membered ring isomeric ruthenacycles containing exocyclic C=C unit.

Mohammad Zafar,[a] Rongala Ramalakshmi,[a] Kriti Pathak,[a] Asif Ahmad,[a] Thierry Roisnel,[b] Sundargopal Ghosh[a]*

Page No. – Page No.

Five-Membered Ruthenacycles: Ligand-Assisted Alkyne Insertion into 1,3-*N,S*-chelated Ruthenium Borate Species